Corrosion behavior of zirconium alloy fuel assembly cladding tubes in the pressurized water reactor's primary circuit

S.N. Orlov,[1,2,3] A.A. Zmitrodan,[1] A.M. Alyoshin[1] and M.Yu. Skripkin[2]*

[1]FSUE "Alexandrov Research Institute of Technology", 72, Koporskoe shosse, 188540 Sosnoviy Bor, Leningrad district, Russian Federation
[2]Saint-Petersburg State University, 7/9 Universitetskaya Emb., 199034 St. Petersburg, Russian Federation
[3]Peter the Great St. Petersburg Polytechnic University (SPbSU), 29, Polytechnischeskaya, 195251 St. Petersburg, Russian Federation
*E-mail: m.skripkin@spbu.ru

Abstract

The corrosion behavior of fuel assembly cladding tubes made of E-110 niobium-containing zirconium alloy is described. Experimental data were obtained during operation and post-operation examination of the KLT-40S reactor. This type of reactor is employed in nuclear-powered icebreakers and the Academic Lomonosov floating nuclear power plant. The data show that the fuel assembly cladding tube material underwent a local (nodular) corrosion in the same way as corrosion of fuel cladding made of E-110 alloy. However, the rate of corrosion of the fuel assembly tubes was significantly lower than that of the cladding of fuel pins, which is explained by a lower heat flux through their surface. A short period of an increase in the rate of corrosion of the fuel assembly tubes was observed during operation of the nuclear propulsion reactor, which was due to a mechanical damage of the protective oxide film on the E-110 alloy surface. As a result, increased concentrations of insoluble zirconium-containing particles, hydrogen and ammonia in the primary coolant were observed during reactor power operation. After the reactor was shut down and the coolant was partially replaced, intense corrosion of the zirconium alloy stopped, indicating self-healing of the protective oxide film on E-110 alloy under the primary coolant conditions.

1. Introduction

The E-110 zirconium alloy (99% zirconium, 0.9–1.1% niobium) is a standard structural material of fuel pin cladding and fuel assembly cladding tubes used in Russian nuclear-powered icebreakers [1]. During operation, this alloy corrodes in the coolant water, possibly leading to a shorter operating life-time of the reactor core [2].

Corrosion of the zirconium alloy in the primary circuits of nuclear propulsion reactors leads to generation of hydrogen in reaction (1):

$$Zr + 2H_2O \rightarrow ZrO_2 + 2H_2 \qquad (1)$$

since ammonia water chemistry regime based on reversible equilibrium reaction (2)

$$2NH_3 \leftrightarrow N_2 + 3H_2 \qquad (2)$$

is maintained in the primary coolant [3], appearance of the additional hydrogen source in the circuit leads to an increase in the ammonia concentration.

As a result, the ammonia concentration in the coolant can exceed the rated limit value. This situation often occurs in the primary circuits of nuclear reactors on *Sevmorput'* nuclear lash lighter carrier and *Soviet Union* icebreaker [4].

The coolant pH and redox values depend on the ammonia concentration. These values determine in their turn the stability of protective oxide films on the structural materials and mass-exchange properties of impurities in the coolant. A change in the mentioned values caused by exceeded limit of ammonia concentration in the coolant can lead to adverse effects.

The corrosion mechanism of zirconium alloys in light-water reactor coolants is rather complex. First, a layer of black non-stoichiometric oxygen-deficient oxide, ZrO_{2-x}, forms on the alloy-oxide film interface; this layer has a protective function [5]. The protective properties of this layer are well expressed that makes it possible to apply ZrO_{2-x} for corrosion prevention of other materials [6]

Upon increase in the oxygen content in the film a layer of white porous stoichiometric oxide, ZrO_2, begins to form on the ZrO_{2-x} surface; this new layer does not have protective functions [7, 8]. Crystallographically, the oxide film consists of two phases. One is a monoclinic phase and the other is a tetragonal phase [9, 10]. This heterogeneity determines the mechanical instability of the film.

The corrosion rate of zirconium alloys suddenly increases after the oxide film thickness grows to about 5 μm [11]. This phenomenon of dramatic increase in corrosion rate is called the breakpoint. Most researchers decide that the breakpoint results from a loss of stability of the protective black non-stoichiometric oxide film. Some researchers consider corrosion of zirconium alloys as a cyclic process: after the oxide film becomes unstable, a new protective layer of black non-stoichiometric oxide forms on the zirconium alloy surface, the corrosion rate appreciably decreases, and the layer of white stoichiometric oxide is released into the coolant. Then the process is repeated and, as a result, the thickness of the film on fuel pins is never larger than 5 μm [12].

The situation is different for niobium-containing zirconium alloys (E-110, E-125) used in Russian-design reactors where no cyclic nature of corrosion is observed. Maroto *et al.* [13] explain the absence of cyclic pattern in the corrosion development of niobium-containing zirconium alloys by growth of protrusions coinciding with the β-Zr phase filaments in these alloys. Since the corrosion rate of β-Zr is higher than that of α-Zr, the protrusions grow faster than the other part of the oxide film; when the film thickness exceeds the damage limit of 5 μm for dioxide protective films, the crests merge to form regions of accelerated corrosion rate, impeding the self-healing of the protective film.

Post-irradiation examination of standard fuel assemblies from reactors of several nuclear-powered icebreakers has shown hot spot corrosion on the E-110 alloy cladding of fuel pins [2]. Significant acceleration of the oxide film growth is associated with the crevice and contact corrosion mechanisms. Specifically, the corrosion rate of alloys is accelerated at the points of contact with the spacer grid where the oxide film is 2–7 times thicker than on the other parts of the surface. It is this local (nodular) corrosion mechanism that is likely responsible for the rise of ammonia and hydrogen concentrations in the primary circuits of icebreaker nuclear reactors.

This paper analyzes the experience in operation of a nuclear propulsion reactor plant where the E-110 alloy was used only as the material for fuel assembly cladding tubes. Changes in the coolant chemical composition, water and gas chemistry regime during the reactor operation are evaluated. Parameters indicating the corrosion enhancement of the zirconium alloy are studied and the surface appearance and composition of crud on the fuel assembly tubes after the reactor shutdown is examined. Based on the data obtained, the corrosion mechanism and characteristics of the process for of E-110 zirconium alloy as a structural material is compared for fuel pin cladding and fuel assembly cladding tubes.

2. Experimental

All data presented in the paper were obtained from operation of the KLT-40S nuclear propulsion reactor plant.

The concentration of gases in the coolant was measured by gas chromatography using the Crystall-2000M instrument after the gases were separated from water samples.

Gases dissolved in the coolant were collected by separating the liquid and gas phases that were formed at near-equilibrium conditions after reducing the sample pressure and temperature. The residual gas content of the coolant sample after degassing (gas concentration being at least 1 nl/kg) was a maximum of 3% of the total value. The total gas content in the coolant sample was estimated using the volumetric gas analysis method.

The ammonia concentration was determined by photometry using a ZOMZ KFK-3-01 photoelectric colorimeter.

The coolant pH was measured by potentiometric method at 25°C using an I-160MI ion meter.

Zirconium oxo-hydroxo species present in the coolant were separated by a cellulose acetate filter and then total zirconium concentration was measured by X-ray fluorescence analysis using the "Spectroscan" analyzer. Morphology of zirconium particles on the filter was examined by electron microscopy using a Nova NanoSEM 450 instrument, the average composition of the particles was analyzed by X-ray microspectroscopy using a Quantax 400 system. The specific activity of radionuclides in the samples was measured by gamma spectrometry using a Gamma-1P spectrometer.

The composition of deposits on the fuel assembly cladding tubes was analyzed on surface wipes obtained after the reactor shutdown. Surface wipe samples were collected using lint-free (madapolam) cloth and PU foam pads moistened with ethanol, which were

pressed onto the surface of interest. The wipe area was 50 cm² or 150 cm². The radionuclide composition of the wipe samples and the composition of corrosion products in the deposits were determined by gamma-spectrometry and X-ray fluorescence analysis, respectively. Visual examination and photographing of the deposits on the fuel assembly surface were performed in parallel with the composition analyses. The analysis work was carried out two years after the decommissioning of the reactor.

3. Results

3.1. Water and gas chemistry of the primary coolant

The water and gas chemistry regime of the primary coolant was highly stable throughout most of the reactor operation time. The ammonia concentration was within 18–60 mg/kg (40 mg/kg on average) and the pH (at 25°C) was from 9.8 to 10.4 (10.2 on average).

The major gases dissolved in the coolant were nitrogen (94–95 vol.%) and hydrogen (4–5 vol.%) with 0.2 vol.% of other gases, such as helium and hydrocarbons.

After the reactor was shut down, the hydrogen fraction increased from 5% to 7 vol.%. This increase was due to a decrease in the average concentration of nitrogen in the coolant (from 0.067 mol/kg to 0.049 mol/kg) and total gas content. A similar decrease in the nitrogen content of the coolant after reactor shutdown without depressurization from 1.8 nl/kg (0.0804 mol/kg) to 0.8–1.0 nl/kg (0.036–0.045 mol/kg) was reported by Kasperovich *et al.* [14]. However, the hydrogen concentration in the coolant before and after the shutdown remained at the same level (0.003 mol/kg).

The concentration relationship between ammonia and gaseous products in the primary coolant can be described by equation (3) given in [15]:

$$[\mathrm{NH_3}] = K \cdot [\mathrm{H_2}]^n \cdot [\mathrm{N_2}]^m \tag{3},$$

where [NH₃], [H₂], and [N₂] are the concentrations of ammonia, hydrogen, and nitrogen, respectively, mol/kg; n, m are empirical coefficients; K is a coefficient depending on the reactor operating power.

The values of K, n and m coefficients calculated based on experimental data are given in Table 1.

Table 1. Coefficients of equation 3 obtained from experimental data.

Reactor operation power, % of nominal value	K	n	m
0	0.36		
30	0.26	0.64	0.34
60	0.2		

The average approximation error of the empirical coefficient values in equation (3) is 16% [16].

3.2. Enhancement of zirconium alloy corrosion process

The enhancement of the zirconium alloy corrosion rate in the primary circuit of the nuclear propulsion reactor plant was observed after repair work was done on the plant. After one month from completion of the work and start of power operation, zirconium concentration of 6–8 µg/kg was observed in the coolant. Zirconium is mostly present in the coolant in the form of insoluble particles (about 95%).

The morphology of zirconium-containing particles separated from the coolant samples is shown in Figure 1. Note that other steel corrosion products, such as oxohydroxo forms of iron, nickel, and chromium, form joint oxides with spinel structure, while zirconium in the coolant forms an independent phase – white particles with molecular formula ZrO_2.

A noticeable change in the ^{95}Zr activity in the coolant was observed at three months after increase in the zirconium concentration therein. The average value of the radionuclide activity in the coolant of the reactor at power operation increased nearly twice from $1.6 \cdot 10^3$ Bq/kg to $2.7 \cdot 10^3$ Bq/kg. The slow rise of the ^{95}Zr activity with respect to the zirconium concentration is explained by the time required for the radionuclide buildup due to neutron activation (the equilibrium value of the ^{95}Zr activity is achieved only at 320 days of the reactor power operation).

The occurrence of zirconium-containing particles in the coolant was accompanied by an increase in the hydrogen and ammonia content. The change in their concentrations at reactor power operation is illustrated in Figure 2.
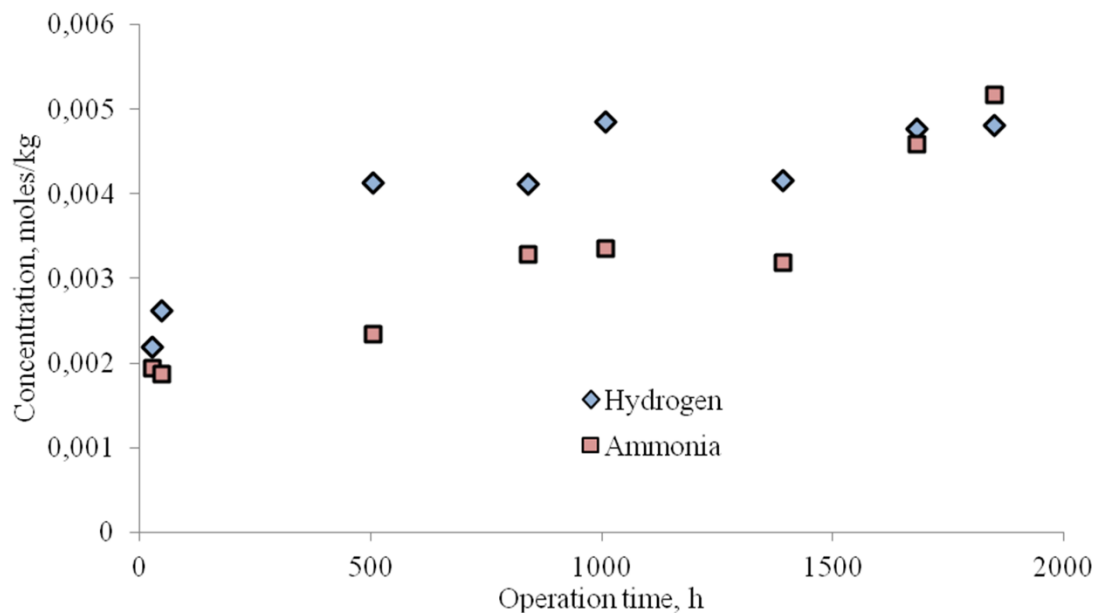

Figure 2. Ammonia and hydrogen concentrations in the coolant of a propulsion nuclear reactor during corrosion enhancement of zirconium alloy.

Figure 2 shows that both hydrogen and ammonia concentrations in the coolant increase upon time of operation. They increase very quickly and after one month of the reactor power operation become two times higher.

The application of equation (3) under enhanced corrosion conditions has produced a large approximation error of 34% [16]. The relationship between the concentrations of ammonia and gaseous compounds under these conditions can be described by empirical equation (4) presented in [17]. The average approximation error of this equation for the enhancement conditions of zirconium alloy corrosion is 19% [16].

$$[H_2] = 1.29[NH_3] + 3.5 \cdot 10^{-4} \tag{4}$$

After the operation cycle with enhanced corrosion of zirconium alloy was over, the coolant was partially replaced to reduce the ammonia concentration, which at that moment reached the limit value according to appropriate water chemistry requirements. After the restart of the reactor power operation, the zirconium concentration in the coolant decreased below the detection limit and did not increased again. The hydrogen and ammonia concentrations in the coolant of the reactor operating at power remained stable throughout the next periods of operation and amounted in average to 68 mg/kg and 6 mg/kg, respectively. In other words, the corrosion rate of the zirconium alloy after the enhancement period returned to initial values.

3.3. Composition of deposits on fuel assembly cladding tubes

Figures 3a and 3b show the surface of selected portions of the fuel assembly cladding tubes corresponding to different areas of the surface.
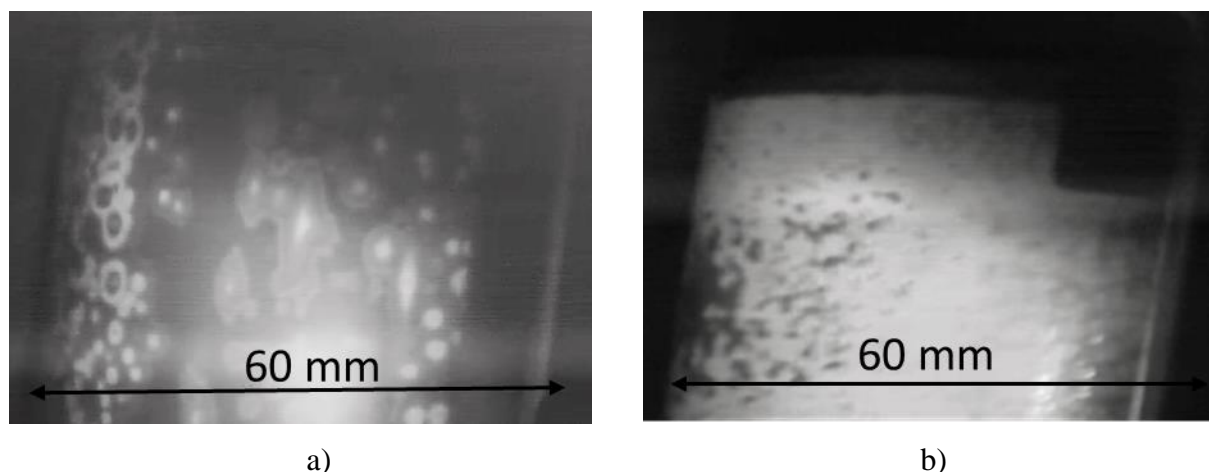

a)   b)

Figure 3. Surface of fuel assembly clad tubes observed after completion of the reactor operation.

It is shown in Figure 3a that rounded spots, nodules of white amorphous ZrO$_2$, are present on the surface of the base metal (or much more likely, on the protective solid black film of zirconium dioxide). Figure 3b shows a more smooth and solid film of amorphous

zirconium dioxide. The occurrence of white lenticular spots is a typical sign of nodular corrosion [11, 18].

The relative elemental composition (percentage of each element in the total amount of corrosion products) of the surface deposits on three fuel assemblies is given in Table 2.

Table 2. Relative elemental composition of surface deposits on fuel assembly cladding tubes.

Test sample	Percentage of element in the total amount of corrosion deposits, wt. %			
	Fe	Cr	Ni	Zr
Fuel assembly 1	4.2	0.2	0.2	95.5
Fuel assembly 2	6.3	0.5	0.4	92.8
Fuel assembly 3	12.7	1.3	2.2	83.8

The data in Table 2 show that loose (removable) deposits on the fuel assembly cladding tubes mainly consist of zirconium dioxide (80–96%). The contamination per unit area of the cladding tube surface with loose zirconium deposits is from 135 $\mu g/cm^2$ to 320 $\mu g/cm^2$ (with respect to zirconium).

The concentration of steel corrosion products (crud) at the cladding tube surface is from 0.015 mg/cm^2 to 0.06 mg/cm^2. Radionuclides produced by corrosion, such as ^{60}Co and ^{54}Mn (^{60}Co: 60–75%,^{54}Mn: 13–25%), are the major contributors to the total activity of samples taken from the surface of the fuel assembly cladding tubes. The contribution of fission products (^{137}Cs, ^{144}Ce, ^{106}Ru, ^{154}Eu) to the total activity is a maximum of 6–10 %. The ^{95}Zr radionuclide has almost completely decayed by the time of sampling.

4. Discussion

The presence of rounded white spots on the surface of fuel assembly cladding tubes made of E-10 alloy is indicative of local (nodular) corrosion that is also observed at the fuel pin cladding [2]. However, corrosion process of zirconium cladding tubes did not affect the water chemistry stability in the primary circuit, except for a short period of enhanced corrosion rate, while corrosion of E-110 cladding did.

This fact points to a lower corrosion rate of fuel assembly cladding tubes than that of fuel pin cladding. Based on the values of unit-area cladding tube contamination (from 0.14 mg/cm^2 to 0.32 mg/cm^2) with zirconium dioxide and contamination density (1600 mg/cm^3 as given in [13]), the thickness of ZrO_2 loose (removable) surface deposits can be calculated. The obtained value is a maximum of 2 µm (average value over the area where the wipe sample is taken), which is much lower than the thickness of the oxide film on fuel pins made of E-110 alloy [1–2].

The low corrosion rate of the cladding tubes can be explained by the 30 times lower heat flux through their surface than through the fuel pin cladding. As is known, the thickness of an oxide film on the E-110 alloy surface exponentially increases with increasing heat flux through it [17].

Low heat fluxes through fuel assembly cladding tubes also explain low crud content on the alloy surface. The deposit thickness calculated using the value of contamination per unit area (from 0.015 mg/cm^2 to 0.06 mg/cm^2) and the crud density in the core (from 1.0 g/cm^3 to 1.2 g/cm^3) [19]) does not exceed 0.3 μm (average over the area where the wipe sample is taken). According to Szabo [20], the presence of crud deposits can be explained by physisorption effects.

Besides a lower corrosion rate, a 3 times smaller surface area of fuel assembly cladding tubes than that of fuel pin cladding may, to a degree, explain the absence of impact of the E-110 cladding tube corrosion on the water chemistry under normal operating conditions.

Enhancement of corrosion process on the fuel assembly cladding tubes was observed after repair work. This was evidently due to a mechanical damage of the protective oxide film on the alloy surface. An important phenomenon is the subsequent self-healing of the oxide film, leading to stabilization of the water chemistry in the primary coolant.

Low concentration and predominant existence as insoluble particles prevent using zirconium concentration in the primary coolant as an indicator of corrosion. The ^{95}Zr specific activity is not suited as a corrosion indicator too because of slow radionuclide generation process not allowing for timely detection of an increase in the corrosion rate. By contrast, a sharp increase of the ammonia and hydrogen concentrations in the coolant due to corrosion of zirconium alloy makes these parameters and their derivatives suited for use as signals of corrosion enhancement [4]. Methodologically, it is convenient to monitor the ammonia concentration in the coolant because ammonia measurement is a routine operation according to applicable water chemistry requirements.

The enhancement of zirconium corrosion is not the only possible cause of a rise of the ammonia concentration in the coolant. However, a sharp increase in this parameter without any changes in the process (such as a change of the plant operating condition, or ammonia or hydrazine addition) shows the necessity to measure other indicative parameters of zirconium alloy corrosion, identify and remove the causes of the corrosion enhancement process.

5. Conclusions

During normal operation of the KLT-40S nuclear propulsion reactor, local (nodal) corrosion of the fuel assembly cladding tubes made of E-110 alloy is observed. This process is slow and does not affect the water chemistry stability.

Enhancement of corrosion on the fuel assembly cladding tubes made of E-110 alloy can be caused by a damage of the protective zirconium dioxide film on the alloy surface. As a result, the concentrations of ammonia and hydrogen in the coolant circuit increase twofold

within one month, thus making these parameters efficient indicators of corrosion enhancement of the zirconium alloy.

The phenomenon of protective oxide film self-healing after damage is observed on the fuel assembly cladding tubes made of E-110 alloy. This effect stops the enhanced corrosion of the alloy and re-establishes stable water chemistry conditions in the coolant.

With the above-mentioned facts, the E-110 alloy is a good choice for making fuel assembly cladding tubes.

Author Statement

S.N. Orlov: conceptualization, investigation, validation, writing–original draft. **A.A. Zmitrodan:** methodology/study design, validation, data curation, supervision project. **A.M. Alyoshin:** software, investigation, data curation. **M.Yu. Skripkin:** validation, formal analysis, writing–review and editing.

Declaration of Competing Interest

The authors declare that they have no known competing financial interests or personal relationships that could have appeared to influence the work reported in this paper.

Acknowledgements

References

1. O.B. Samoilov, D.G. Preobrazhenskii and O.A. Morozova, Results of operation and operating conditions of reactor cores in nuclear-powered icebreakers. Abstract, The 9-th Russian Conference on Reactor Materials, Dimitrovgrad, 2009, 68–70 (in Russian).

2. A.V. Vatulin, I.N. Volkova and A.E. Novoselov, Corrosion of E-635 alloy in nuclear-powered icebreaker reactor core, *Atomic Energy*, 2011, **111**, 235–237. doi: 10.1007/s10512-012-9482-0

3. Water quality requirements for the primary and tertiary circuits of VVER-type KLT-40 reactors in vessels of Russia's Marine Transport Department, Departmental Standard 95 10002-95 RSC "Kurchatov Institute", Moscow, 1995 (in Russian).

4. S.A. Kabakchi, A.V. Luzakov, D.S. Urtenov, E.A. Katanova, I.A. Gasai and A.E. Verkhovskii, Assessment of the corrosion of elements in the equipment of the primary circuit of marine propulsion power units using characteristics of applicable water chemistry, *Thermal Engineering*, 2019, **66**, 183–188. doi: 10.1134/S0040601519030030

5. V.G. Kritskii, Yu.A. Radionov, I.G. Berezina, E.V. Zelenina, A.V. Gavrilov, A.P. Shchukin, A.I. Fedorov, M.G. Shchedrin and A.V. Galanin, Formation and removal of deposits in the VVER NPP primary circuit, Beresta, Saint-Petersburg, 2011 (in Russian).

6. A.O. Al-Roubaiy, H.H.J. Jamal Al-Deen and M.S. Tuma, Effect of ZrO_2 addition on the corrosion resistance of gallium-based restorative, *Int. J. Corros. Scale Inhib.*, 2020, **9**, no. 3, 1121–1141. doi: [10.17675/2305-6894-2020-9-3-22](10.17675/2305-6894-2020-9-3-22)

7. J.S. Moya, M. Diaz, J.F. Bartolome, E. Roman, J.L. Sacedon and J. Izquierdo, Zirconium oxide film formation on zircaloy by water corrosion, *Acta Mater.*, 2000, **48**, 4749–4754. doi: [10.1016/S1359-6454(00)00267-6](10.1016/S1359-6454(00)00267-6)

8. W. Cin, C. Nam, H.L. Li and J.A. Szpunar, Tetragonal phase stability in ZrO_2 film formed on zirconium alloy and its effects on corrosion resistance, *Acta Mater.*, 2007, **55**, 1695–1701. doi: 10.1016/j.actamat.2006.10.030

9. M.G. Glavicic, J.A. Szpunar and Y.P. Lin, A method for the quantitative phase analysis of ZrO_2 films grown on Zr-2.5% Nb pressure tubes, *J. Nucl. Mater.*, 1997, **245**, 147–151. doi: [10.1016/S0022-3115(97)00017-2](10.1016/S0022-3115(97)00017-2)

10. B. Cox, A new model for the in-reactor corrosion of zirconium alloys, Technical Committee meeting, *Influence of water chemistry on fuel cladding behavior*, 1993.

11. A.Yu. Melehovets and I.V. Pyshin, Corrosion mechanisms of VVER fuel cladding, (Review), VANT, *Nuclear reactor physics*, 2019, **3**, 67–85.

12. G.P. Sabol, ZIRLO: an alloy development, *J. ASTM Int.*, 2005, **2**. doi: [10.1520/JAI12942](10.1520/JAI12942)

13. A.J.G. Maroto, R. Bordoni, M. Villegas, A.M. Olmedo, M.A. Blesa, A. Iglesias and P. Koenig, Growth and characterization of oxide layers on zirconium alloys, *J. Nucl. Mater.*, 1996, **229**, 79–92. doi: [10.1016/0022-3115(95)00233-2](10.1016/0022-3115(95)00233-2)

14. A.I. Kasperovich, B.I. Kolesov and N.G. Sandler, Water-chemical processes in reactor units of nuclear icebreakers and floating power units, *Atomic Energy*, 1996, **81**, 261–266.

15. D.D. Korotayeva, I.N. Kulakov and A.N. Lepekhin, Numerical analysis of ammonia water and gas chemistry parameters in the primary circuit of the KLT-40S reactor on a Project 20870 floating power unit, Proceedings of IX KOMANDA Workshop of young nuclear scientists and engineers, Saint-Petersburg, 2021, 153–155 (in Russian).

16. S.N. Orlov, A.A. Zmitrodan and E.E. Shcherbakov, Numerical simulation of the ammonia and gaseous product concentrations in the primary coolant of nuclear marine reactors, nuclear propulsion reactor plants, *Life cycle management technologies* (in press).

17. A.V. Bulanov, B.I. Kolesov, M.L. Lukashenko, A.M. Hudiakov, S.A. Kabakchi and O.P. Arkhipov, The radiolysis of ammonia in the primary coolant of floating nuclear power units, *Atomic Energy*, 2000, **88**, 368–372. doi: [10.1007/BF02680531](10.1007/BF02680531)

18. V.G. Kritskii and B.A. Kalin, Fuel pin cladding corrosion during the life cycle of fuel assemblies in light water reactors, MIFI, Moscow, 2020.

19. R.F. Hazelton, *Characteristics of fuel crud and its impact on storage, handling, and shipment of spent fuel*, Research report, Pacific Northwest Laboratory, Richland, 1987.
20. S. Szabó, Metal corrosion and its relation to other fields of science, *Int. J. Corros. Scale Inhib.*, 2015, **4**, no. 1, 35–48. doi: 10.17675/2305-6894-2015-4-1-035-048

♦ ♦ ♦